Electromagnetic Design of a Spiral Surface RF-Coil Transceiver for NQR-based explosive detection in the humanitarian demining setting

P. Farantatos[1], J. Barras[1], I. Poplett[1], P. Kosmas[1]
1. Department of Informatics & Robotics, Humanitarian Technologies Lab, King's College London, London, United Kingdom

Introduction

Landmines are a major problem of international concern and it is therefore crucial to detect them with high probability of success. Nuclear Quadrupole Resonance (NQR) is a radiofrequency spectroscopic technique where explosive substances can be detected through the application of AC magnetic field transmission pulses at particular resonant frequencies specific to the target explosive's material. By detecting the magnetic resonance signal emitted from the target material during its relaxation, its substance can be remotely inspected. A common substance present in explosives is the nitrogen-14 nucleus, which is possible to detect through the use of NQR at transition frequencies in the range of 0.5-5 MHz. A substitute substance that can be safely utilized for conceptual NQR system design studies is sodium nitrite; its detection frequency is at 3.41 MHz.

Our group is currently developing the world's first low-cost, rugged and portable NQR system for anti-vehicle mines (AVMs) detection in the humanitarian demining setting. Major component of the system is its probe transceiver which comprises a spiral RF-coil operating in the near field. The coil is matched to the frequency of interest with a capacitor parallel to its terminals, creating a parallel resonant LC circuit.

In order to adapt to the humanitarian demining setting's functional requirements, the sizing of the coil is designed to be proportional to an AVM size, leading to a coil diameter of approximately 400 mm. Additionally, the coil is constructed from commercially available copper tube of an external diameter of 8 mm and a thickness of 2 mm, ensuring low weight and low cost as well as the simplification of the coil's manufacturing sophistication.

COMSOL Multiphysics [1] is utilized for the conceptual electromagnetic design of the spiral coil and the comparative evaluation of its performance with respect to different geometrical specifications and operational conditions.

Geometrical Set-up and Materials

The spiral coil is geometrically set up as the difference of two helical coils with zero axial pitch, 5 turns and represented by a Bézier curve with a relative tolerance of 1E-5. The geometrical parameters of interest that are under investigation are its major radius (r) and the radial pitch (p). Copper was chosen for the coil tube material.

At the coil's end caps, rectangular surfaces are connected that represent the coil terminals. The two rectangles that intercede with the terminals represent the parallel configuration of the excitation port and a parallel matching capacitor (Fig.1).

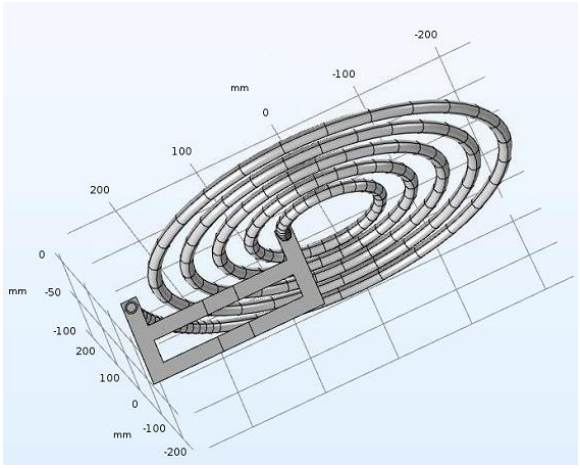

Figure 1. Geometrical representation of the spiral coil with its end cap terminals, excitation port and matching capacitor.

The coil set-up is encapsulated by an air sphere with a radius of a 1000 mm and a layer section of 100 mm, defined as a Perfectly Matched Layer (PML), in order to simulate ideal conditions with respect to outgoing energy absorption and avoidance of spurious reflections (Fig. 2).

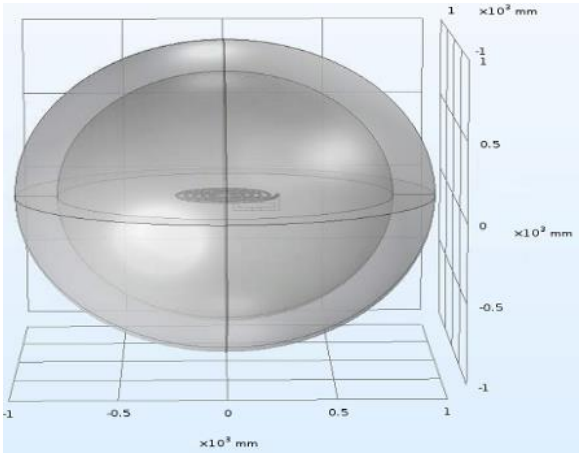

Figure 2. The coil is encapsulated by an air sphere of a radius of 1000 mm and a PML with a layer of 100 mm.

Numerical Model Set-Up

For the numerical simulation of the model, the RF module is utilized. In particular, in order to calculate the response of the model subject to harmonic excitation, the Frequency Domain study is utilized as well as the Adaptive Frequency Sweep for a finer frequency resolution.

The wave equation (1) governs the air sphere domain, the PML, as well as the copper tube thickness domain. The hollow tube domain that in reality comprises air is excluded from the calculations, as there is no added design value in calculating magnetic field distributions outside of the detection area of interest. This way, computational costs are further reduced.

$$\nabla \times \mu_r^{-1}(\nabla \times \mathbf{E}) - k_0^2\left(\epsilon_r - \frac{j\sigma}{\omega\epsilon_0}\right)\mathbf{E} = \mathbf{0} \quad (1)$$

The coil boundary is governed by an Impedance Boundary Condition (2), in order to take into account conductive surface losses at the coil domain.

$$\sqrt{\frac{\mu_0\mu_r}{\epsilon_0\epsilon_r - j\sigma/\omega}}\,\mathbf{n}\times\mathbf{H} + \mathbf{E} - (\mathbf{n}\cdot\mathbf{E})\mathbf{n} = (\mathbf{n}\cdot\mathbf{E}_s)\mathbf{n} - \mathbf{E}_s \quad (2)$$

In order to represent the coil terminals, lossless metallic conductors connecting the excitation port to the coil's end caps by exploiting the Perfect Electric Conductor (PEC) boundary condition (3) are added.

$$\mathbf{n}\times\mathbf{E} = \mathbf{0} \quad (3)$$

For harmonically exciting the coil, a uniform inport lumped port is defined at the intersection of the metallic coil terminals (PEC) with a characteristic impedance of 50 Ohm. Its terminal is of cable type for providing a voltage-driven transmission line of a modulated Gaussian pulse per frequency sweep. The target simulation frequency is 3.4 MHz, which is close to the sodium nitrite detection frequency value (3.41 MHz); this frequency difference does pose any loss of generality in the validity of the simulation results, as a difference of 0.01 MHz is negligible with respect to the radiation characteristics for comparatively evaluating different coil geometries. Finally, in order to investigate impedance matching to 3.4 MHz, a uniform lumped capacitive element is added parallel to the lumped port at the intersection of the PEC boundaries.

Preliminary Mesh Sensitivity Analysis

On a preliminary stage and prior to engaging to the final geometrical model creation and calculation of electromagnetic parameters, a preliminary mesh sensitivity analysis was conducted in order to define the mesh values that would provide the trade-off between computational time and accuracy of results. To that end, a global mesh parameter was defined (h1) and fractionally allocated to all the domains and boundaries of a larger model, but with comparable dimensions to our final parametrized model: a spiral coil with 7 turns, major radius of 35 mm, radial pitch of 70 mm and an air sphere of 2000 mm radius with a PML layer of 200 mm. A matching capacitor of 250 pF was also allocated. In order to evaluate the final value of h1, a parametric Frequency Domain study was launched with respect to the absolute value of the port impedance result for parametrized values of h1 ranging from 1-5 mm with a step size of 1 mm. The maximum value that would not significantly compromise the resulting port impedance value was found to be h1=5 mm (Fig. 3).

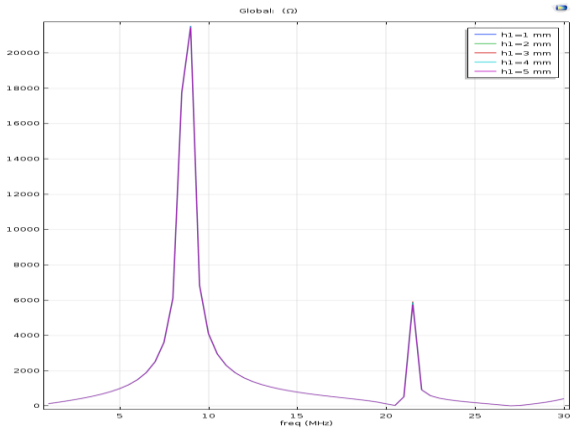

Figure 3. Absolute value of port's impedance for a range of values for mesh parameter h1.

Analysis Steps

Firstly, in order to roughly find resonant modes for different coil geometries a Frequency Domain study was launched with a step size of 1 MHz. Subsequently, more accurate resonant modes were found with the use of Adaptive Frequency Sweeps of a step size of 0.01 MHz.

The different models were matched to the frequency region of 3.4 MHz (which is the relevant frequency region of interest for NQR detection) by activating the capacitive element parallel to the lumped port. Table 1 shows the different model configurations.

Table 1. Different models cases studied:

Model name	Major Radius (r) [mm]	Radial Pitch (p) [mm]	Resonant frequency [MHz]	Capacitor matching around 3.4 MHz [pF]
r25p40	25	40	84	454
r50p40	50	40	71	336
r100p40	100	40	95	208
r100p30	100	30	109	235
r125p20	125	20	110	202

For each model, the imaginary part of the magnetic flux component vertical to the coil plane (Bz) was calculated, as the magnetic fields are 90 degrees out of phase with respect to the electric potential applied by the lumped port. The geometrical locus of the exported Bz values was defined as the line that extended vertically to the coil plane from the coil's geometrical center to a distance of 400 mm (Fig. 4).

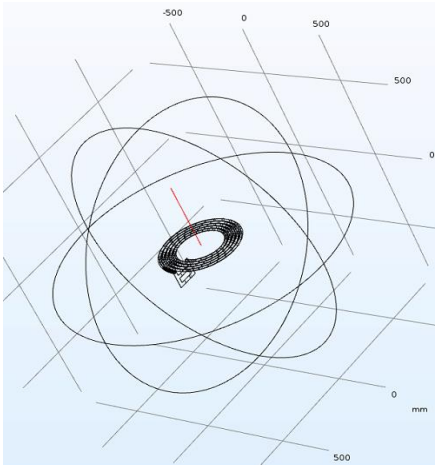

Figure 4. Geometrical locus (red line) of the exported magnetic flux component, Bz.

After exporting the Bz values, the normalized magnetic field decay along the line was calculated as a percentage fraction of the magnetic field value at the coil center: $Bnorm[\%] = B_z \times 100/B_{center}$

The models are comparatively evaluated along with an experimental prototype constructed in our lab.

Additionally, the absolute value of the port impedance is comparatively evaluated per model.

Finally, the normalized magnetic field decay and absolute port impedance calculations are repeated for the r25p40 model, which is as close dimensionally to the prototype coil developed as possible, in two operational conditions: a) Operation under a shielded aluminum box and b) operation with metallic debris present at the detection region.

Although the coil under design is a transceiver coil, it is configured as a transmitter only in our simulations. The rationale behind this approach lies on the exploitation of the "reciprocity theorem": Practically, the contribution to the received signal from a sample substance is proportional to the magnetic field at the same position if the same coil is used as a transmitter [3].

Results: Port Impedance

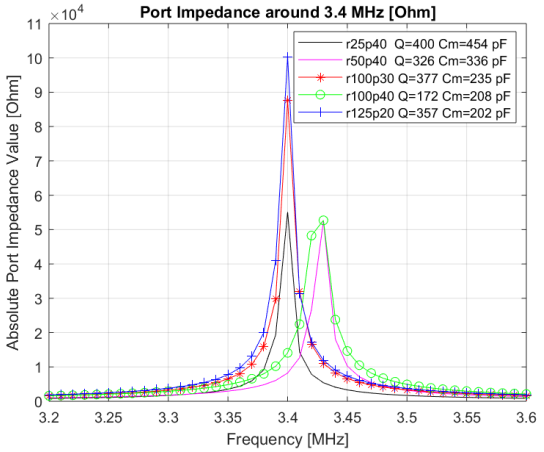

Figure 5. Absolute value of the port impedance matched at the frequency region of 3.4 MHz.

Fig. 5 depicts the different values of the port impedance per model case. The coil with the matching capacitor is treated as a parallel resonant circuit, where impedance peaks at resonance. The bandwidth of the impedance curve is measured between the half power points and corresponds to the 70.7% of the maximum impedance value.

Results: Normalized Magnetic Field Decay and Comparison with Experimental Field Mapping on a Prototype Coil

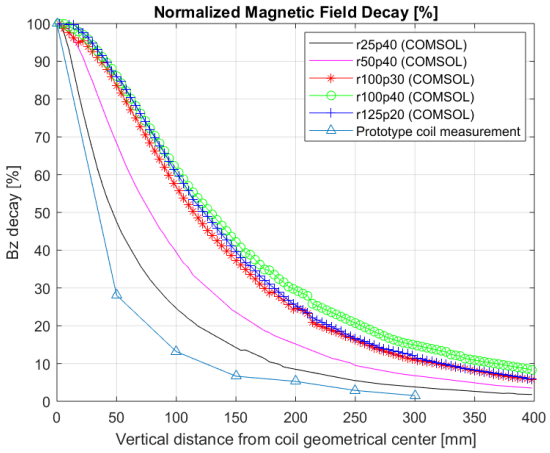

Figure 6. Normalized magnetic field decay [%] from the coil's geometrical center.

Fig. 6 depicts the normalized magnetic field decay as a fractional percentage drop from the magnetic field value at the geometrical center of the coil. Model r25p40 which is closer to its geometrical specifications as the prototype coil constructed shows the closest behavior to the experimental measurement.

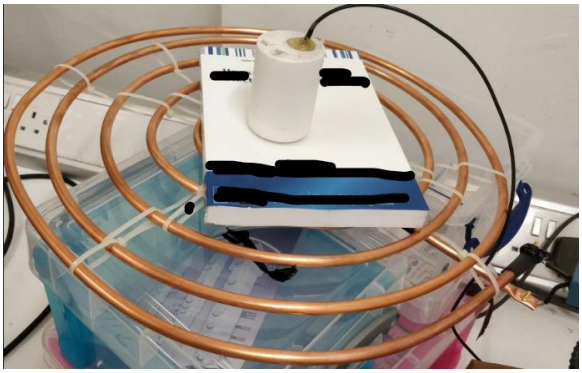

Figure 7. The prototype coil used for comparing the normalized magnetic field decay values.

Fig. 7 depicts the prototype coil that was utilized for experimental verification of the simulation results. A function generator at 3.6 MHz connected to a TOMCO class AB amplifier was used for exciting the coil. The magnetic field mapping values were measured with a magnetic field probe (white cylindrical structure) inside a shielded aluminum box in order to avoid external RF interference.

Results: Shielding Box Encapsulation and Presence of Metallic Debris Effects

In order to investigate the effect to the coil's performance when the coil is encapsulated by a shielded aluminum box, an aluminum cube of a side length of 700 mm and a thickness of 2 mm was added for surrounding the coil in model case r25p40 (Fig. 8).

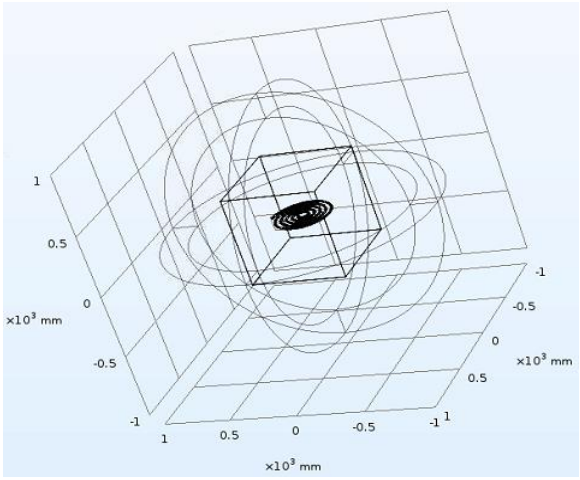

Figure 8. r24p40 with an added aluminum encapsulation.

Additionally, a simulation with the same model case, r25p40 was conducted in order to determine the effect on the coil's performance of the presence of small metallic debris of copper material in the detection area, as Fig. 9 depicts.

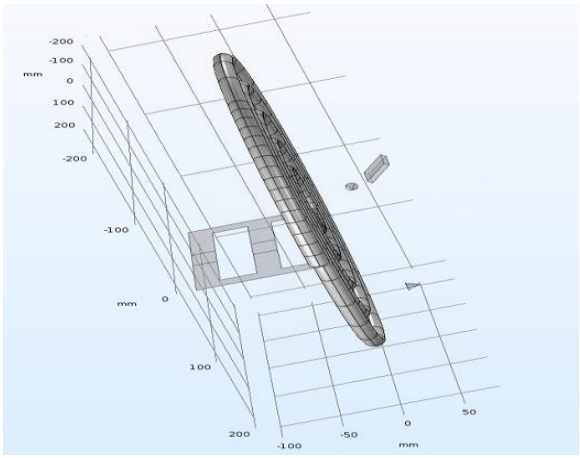

Figure 9. Model case r25p40 with added metallic debris. Two conical copper structures of a bottom radius, height and top radius of 5 mm, 10 mm and 0.5 mm respectively are added 50 mm away vertically from the coil plane and at a planar position of 100 mm away from the coil's center. Additionally, a rectangular metallic structure of width, depth and height of 30 mm, 5 mm and 40 mm respectively is added at a vertical distance of 70 mm from the coil center and at a planar position of 40 mm away from the coil's center.

Interestingly, the comparative port impedance values for model case r25p40 indicate that the encapsulation of the coil by an aluminum box shifted the resonant point of the coil about 0.1 MHz (Fig. 10). The presence of metallic debris in the detection area, on the other hand, led to a slight increase of the Q-factor.

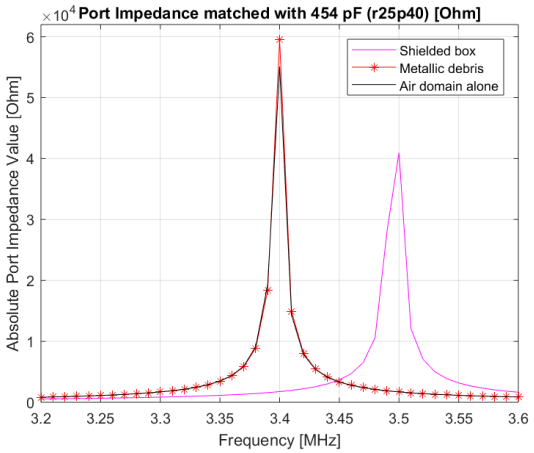

Figure 10. Model case r25p40 comparative port impedance calculation graph at the presence of a shielding box and metallic debris.

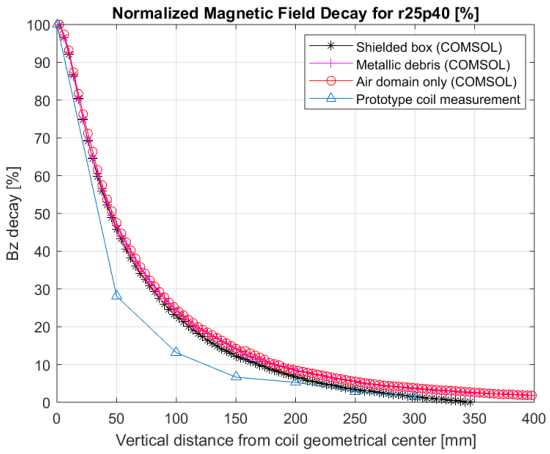

Figure 11. Model case r25p40 comparative normalized magnetic field decay from the coil center at the presence of a shielding box and metallic debris.

Fig. 11 depicts the comparative normalized field decay between the different operational conditions as well as the experimental measurement. The numerical simulations show very limited differences in the magnetic field behavior at the different operational conditions.

Conclusions and Future Work

In the present report, the conceptual electromagnetic design steps for an NQR-based spiral RF-coil transceiver for explosive materials detection were presented.

Overall, model r100p40 bears the best performance results; its Q-factor is around 172 indicating better resilience against RF interference for in field operation. Although a higher Q-factor would ostensibly seem beneficial for the coil design, its susceptibility to noise sources would equivalently increase, which would be a functional risk during in field operation. Additionally, it is evident that the increase of the coil's major radius leads to approximately twice as much magnetic field quality conservation.

Model r25p40 that has its geometry similarly defined as the experimental prototype coil, shows the closest behavior regarding magnetic field quality decay from the coil center, which demonstrates the consistency of the relative magnetic field decay patterns obtained through numerical simulation with respect to a realistic implementation. Be that as it may, it has to be taken into account that the model simulated is analyzed in noise-free conditions and with a mathematically perfect mechanical structure. The experimental coil prototype is susceptible to manufacturing and geometrical imperfections, as well as RF interference and additional accumulated instrumental circuit noise; it is intended to be low-cost and easy to manufacture, suitable for the humanitarian demining setting.

As far as operation under a shielding box in model r25p40 is concerned, the encapsulation of a conductive block loads the coil to a point where there is a 0.1 MHz frequency shift. Further investigation is necessary regarding the bandwidth resilience levels when the coil is operating under a shielding box with respect to different geometrical designs and shielding box structure sizes.

Regarding the presence of metallic debris at the coil detection area, this led to a slight increase of the Q-factor, but this is not a conclusive result; further investigation is necessary with respect to the size and positioning of metallic debris at the coil plane, as, in reality, coils are susceptible to inductively coupling with nearby metallic objects, leading to operational bandwidth shifts.

Furthermore, an interesting feature to explore in the near future with respect to the optimization of the

spiral coil's geometry is the utilization of the Optimization Module for retrieving optimal geometrical specifications while maximizing the magnetic field quality within the detection area. Also, the magnetic field decay mapping needs to be quantified in additional distances from the coil center in order to fully map the coil's effective detection area. Finally, the AC/DC module's Electrical Circuit interface shall be explored in order to simulate the behavior of the finalized coil model with respect to its driving circuit components.

References

1. "RF Module User's Guide, version 5.3", COMSOL, Inc, www.comsol.com
2. Y. Otagaki, P. Farantatos, W. Rafique, J. Barras, P. Kosmas, Design and development of an NQR-based explosive detection system for humanitarian demining, *Mine Action Symposium Book of Papers*, p.g. 38-41 (2018)
3. E. Fukushima, S.B.W. Roeder, *Experimental Pulse NMR: A nuts and bolts approach*, Addison-Wesley (1981)

Acknowledgements

This work was supported by UK's Engineering and Physical Sciences Research Council (EPSRC) under project grant EP/P02906X/1.

The authors are grateful to Dr. I. Bitharas for his technical insights on COMSOL features. Additionally, the authors would like to thank Dr. M. Rowe for his feedback on NQR coil design. Finally, the authors would like to thank the lab members Dr. N. Payne and Y. Otagaki for their continuous support of the NQR research activity.